

## Supporting Information

### Morphology-Dependent Charge Storage Performance of $\text{Co}_3\text{O}_4$ Nanostructures in All-Solid-State Flexible Supercapacitor

Biraj Kanta Satpathy,<sup>1</sup> Arpan Kumar Nayak,<sup>2</sup> C. Retna Raj,<sup>1,3</sup> and Debabrata Pradhan<sup>1,2</sup>

<sup>1</sup>*School of Nanoscience and Technology, Indian Institute of Technology Kharagpur, Kharagpur 721 302, India*

<sup>2</sup>*Materials Science Centre, Indian Institute of Technology Kharagpur, Kharagpur 721 302, India*

<sup>3</sup>*Department of Chemistry, Indian Institute of Technology Kharagpur, Kharagpur 721 302, India*

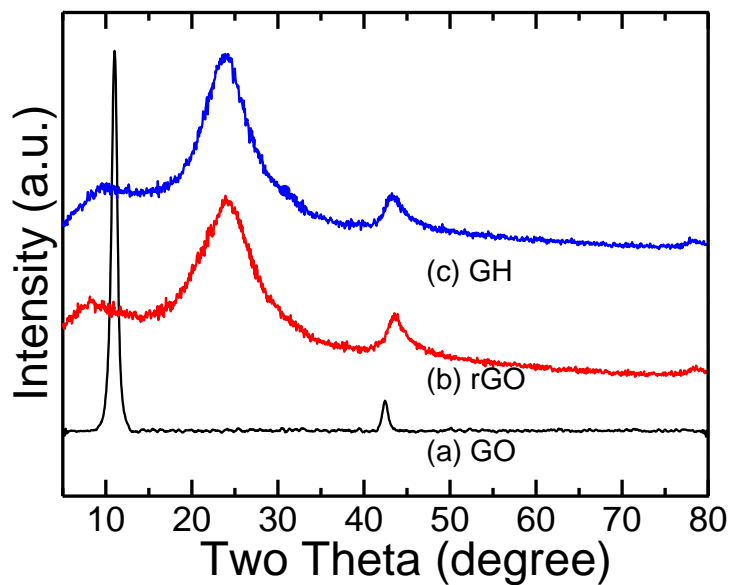


**Fig. S1.** Powder XRD patterns of (a) GO, (b) rGO, and (c) GH. The rGO and GH was obtained by hydrothermal treatment of GO in aqueous solution at 120 and 150 °C for 12 h, respectively.

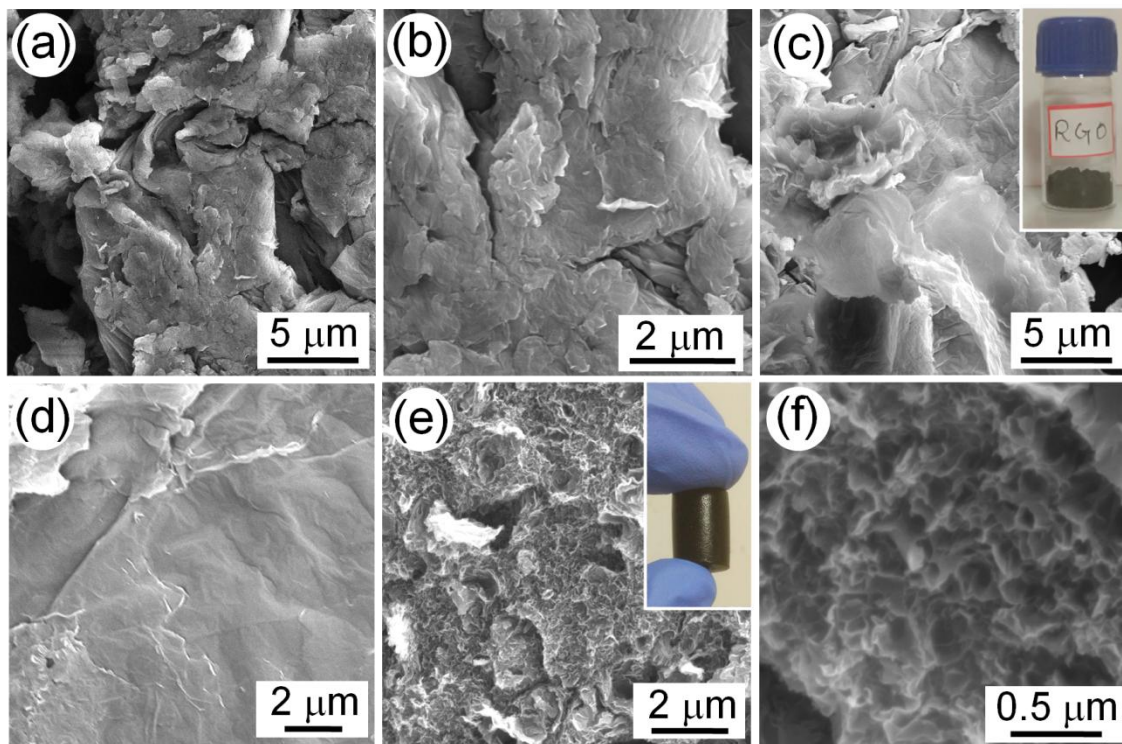


**Fig. S2.** FESEM images of the as-synthesized (a,b) GO, (c,d) rGO, and (e,f) GH. Insets of (c) and (e) show photographs of the corresponding product.

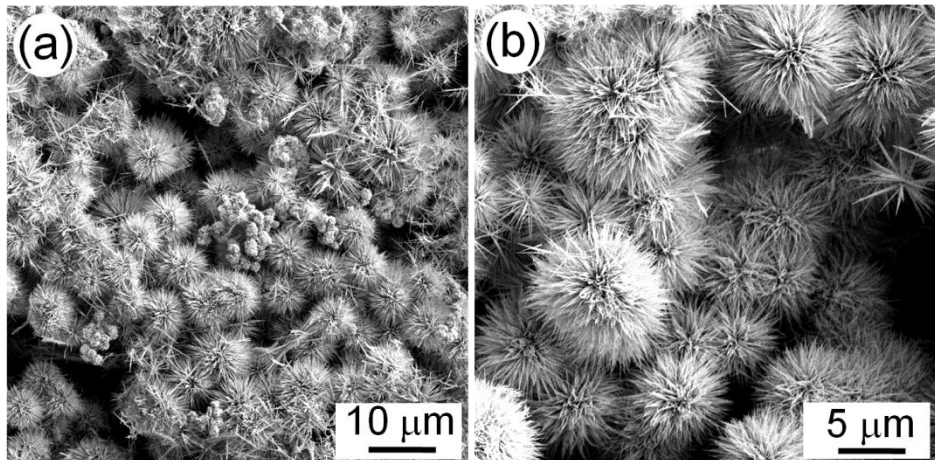


**Fig. S3.** FESEM images of the as-synthesized product at low magnifications obtained by microwave-assisted hydrothermal method at 120 °C.

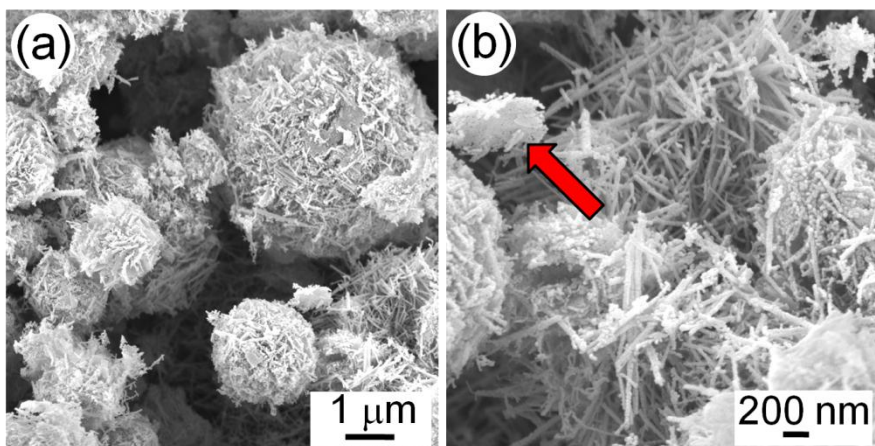


**Fig. S4.** FESEM images of the as-synthesized product obtained by microwave-assisted hydrothermal method at 150 °C. The red color arrow mark in (b) indicates 2D flake-like structure.

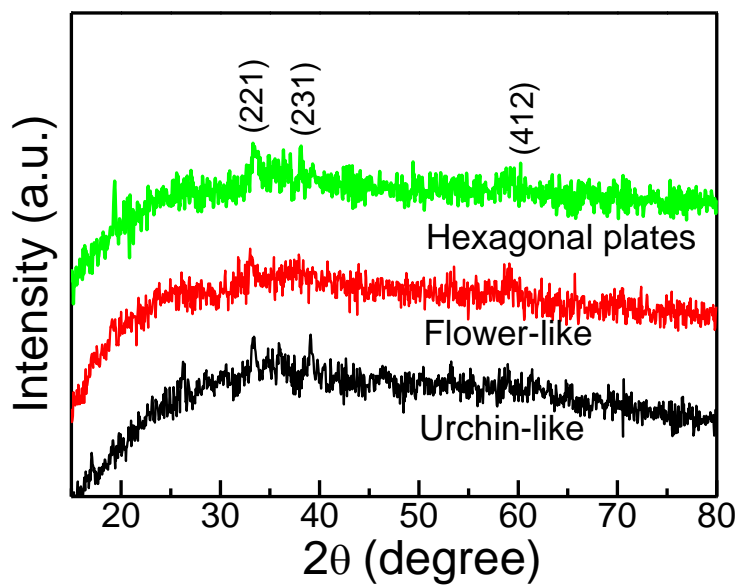


**Fig. S5.** Powder XRD patterns of the as-synthesized products obtained by varying the reaction temperature to form different shapes such as urchin-like ( $120\text{ }^{\circ}\text{C}$ ), flower-like ( $180\text{ }^{\circ}\text{C}$ ) and hexagonal plates ( $200\text{ }^{\circ}\text{C}$ ) with other reaction parameters fixed, i.e.,  $250\text{ W}$  for  $30\text{ min}$  and cobalt and urea molar concentration at  $0.1\text{ M}$ . The XRD pattern is matched with JCPDS file 48-0083 for cobalt carbonate hydroxide hydrate  $[\text{Co}(\text{CO}_3)_{0.5}(\text{OH}) \cdot 0.11\text{H}_2\text{O}]$

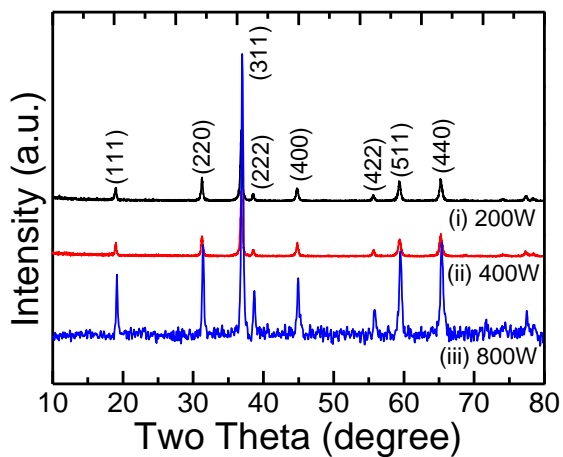


**Fig. S6.** Powder XRD patterns of the products obtained by varying the microwave power and then annealed at  $500\text{ }^{\circ}\text{C}$  under air for  $3\text{ h}$ .

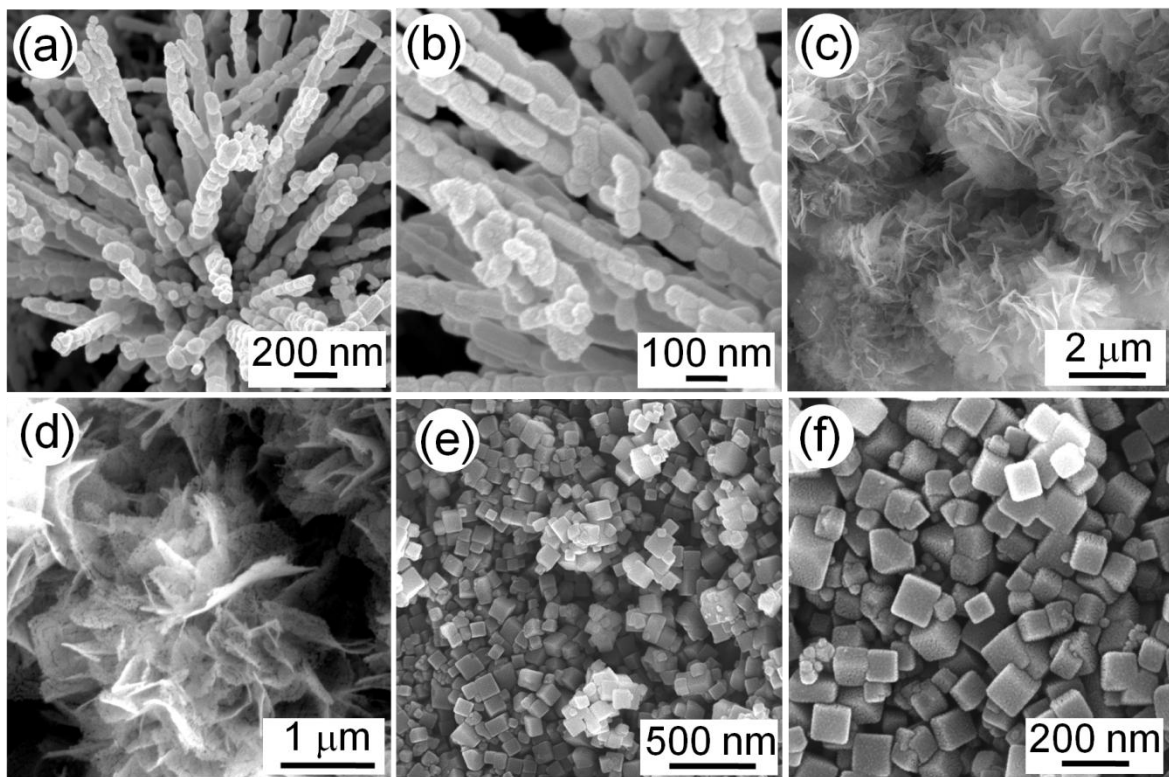


**Fig. S7.** FESEM images of the samples annealed at 500 °C for 3 h. These samples were synthesized by microwave-assisted hydrothermal method by varying the reaction temperature (a,b) 120 °C and (c,d) 180 °C (0.1 M precursors, 400 W 30 min). The images shown in (e,f) were synthesized at 0.01 M precursors at 400 W and 180 °C for 30 min.

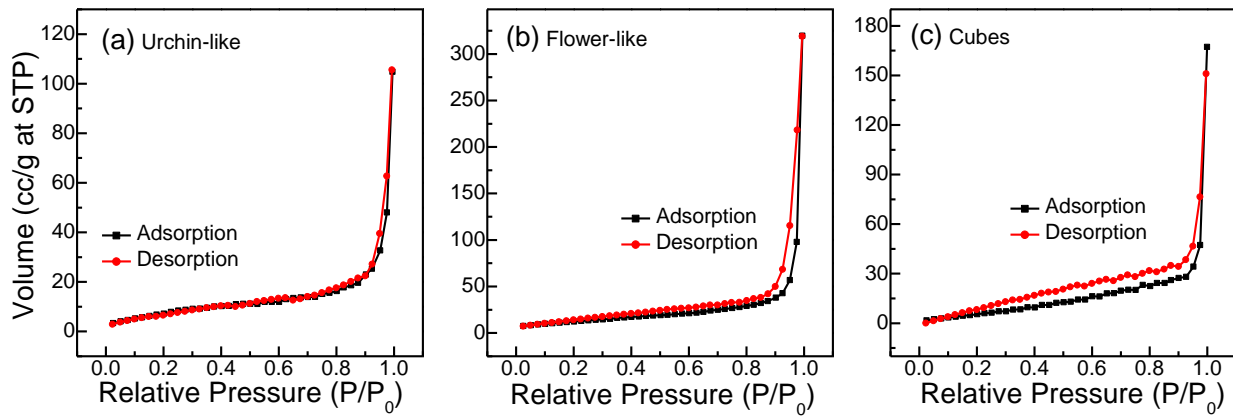


**Fig. S8.** The  $N_2$  adsorption-desorption isotherms of (a) urchin-like, (b) flower-like, and (c) cube morphology of  $\text{Co}_3\text{O}_4$ .

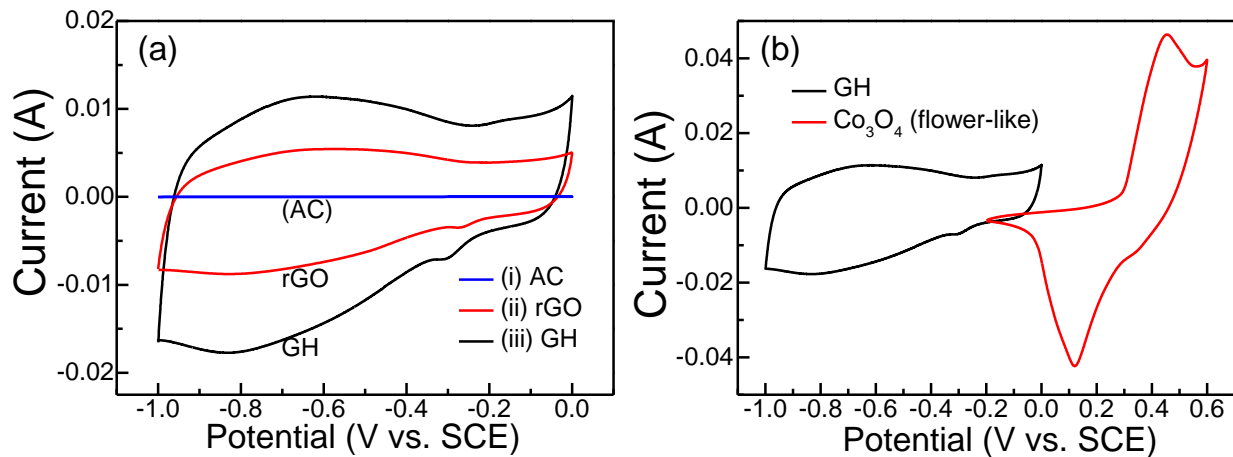


**Fig. S9.** (a) Cyclic voltammograms of (i) AC, (ii) rGO, and (iii) GH at  $10 \text{ mV s}^{-1}$ . (b) Cyclic voltammograms of GH and flower-like  $\text{Co}_3\text{O}_4$  in different potential windows.



**Fig. S10.** Photographs on powering small devices using the fabricated  $\text{Co}_3\text{O}_4/\text{GH}$  ASC device.

Table S1. Comparison on the Supercapacitor Performance of the Reported  $\text{Co}_3\text{O}_4$  based Materials

Electrode Material	Synthesis Process	Electro lyte	$C_s$ from CV	$C_s$ from GCD	Energy Density	Power Density	Ref
$\text{Co}_3\text{O}_4$	Microwave Hydrothermal	2 M KOH	$782.5 \text{ F g}^{-1}$ at $5 \text{ mV s}^{-1}$	$341.5 \text{ F g}^{-1}$ ( $1 \text{ A g}^{-1}$ )	$29 \text{ Wh kg}^{-1}$	$916 \text{ W kg}^{-1}$	This work
$\text{CoO}/\text{Co}_3\text{O}_4$	Hydrothermal	3 M KOH	$436 \text{ F g}^{-1}$ at $5 \text{ mV s}^{-1}$	$451 \text{ F g}^{-1}$ at $1 \text{ A g}^{-1}$	$10.52 \text{ Wh kg}^{-1}$	$140 \text{ W g}^{-1}$	<sup>1</sup>
$\text{Co}_3\text{O}_4$	Laser ablation	0.5 M $\text{H}_3\text{PO}_4$	$177 \text{ F g}^{-1}$ at $1 \text{ mV s}^{-1}$	$172 \text{ F g}^{-1}$ at $0.9 \text{ A g}^{-1}$	$3.01 \text{ Wh kg}^{-1}$	$0.031 \text{ kW g}^{-1}$	<sup>2</sup>
rGO@ $\text{Co}_3\text{O}_4$	Co-precipitation	6 M KOH		$546 \text{ F g}^{-1}$ at $1 \text{ A g}^{-1}$			<sup>3</sup>
CoO nanopillar	Hydrothermal	2 M KOH	$510 \text{ F g}^{-1}$ at $5 \text{ mV s}^{-1}$	$354 \text{ F g}^{-1}$ at $1 \text{ A g}^{-1}$	$21.25 \text{ Wh kg}^{-1}$	$225 \text{ W kg}^{-1}$	<sup>4</sup>
$\text{Co}_3\text{O}_4-\text{rGO}$	Electrodepostion	1 M KOH		$406 \text{ F g}^{-1}$ at $1 \text{ A g}^{-1}$	$23.3 \text{ Wh kg}^{-1}$	$2.3 \text{ kW kg}^{-1}$	<sup>5</sup>
AuNP/nano- $\text{Co}_3\text{O}_4$	In situ reduction	2 M KOH		$681 \text{ F g}^{-1}$ at $0.5 \text{ A g}^{-1}$	$25 \text{ Wh kg}^{-1}$		<sup>6</sup>
$\text{Co}_3\text{O}_4-\text{n}-\text{rGO}$	Hydrothermal	6 M KOH			$3.5 \text{ Wh kg}^{-1}$	$7 \text{ kW kg}^{-1}$	<sup>7</sup>
$\text{Co}_3\text{O}_4@\text{N}-\text{rGO}$	Hydrothermal	2 M KOH		$450 \text{ F g}^{-1}$ at $1 \text{ A g}^{-1}$			<sup>8</sup>

## References

- <sup>1</sup> M. Pang, G. Long, S. Jiang, Y. Ji, W. Han, B. Wang, X. Liu, Y. Xi, D. Wang, and F. Xu, *Chem. Eng. J.*, 2015, **280**, 377–384.
- <sup>2</sup> X. Y. Liu, Y. Q. Gao, and G. W. Yang, *Nanoscale* 2016, **8**, 4227–4235.
- <sup>3</sup> D. Yin, G. Huang, Q. Sun, Q. Li, X. Wang, D. Yuan, C. Wang, and L. Wang, *Electrochim. Acta* 2016, **215**, 410–419.
- <sup>4</sup> Y.-B. Liu, L.-Y. Lin, Y.-Y. Huang, and C.-C. Tu, *J. Power Sources*, 2016, **315**, 23–34.
- <sup>5</sup> M. Qorbani, T.-C. Chou, Y.-H. Lee, S. Samireddi, N. Naseri, A. Ganguly, A. Esfandiar, C.-H. Wang, L.-C. Chen, K.-H. Chen, and A. Z. Moshfegh, *J. Mater. Chem. A*, 2017, **5**, 12569–12577.
- <sup>6</sup> Y. Tan, Y. Liu, L. Kong, L. Kang, and F. Ran, *J. Power Sources*, 2017, **363**, 1–8.
- <sup>7</sup> S. Kalasina, N. Phattharasupakun, M. Suksomboon, K. Kongsawatvoragul, and M. Sawangphruk, *Electrochim. Acta*, 2018, **283**, 1125–1133.
- <sup>8</sup> R. Atchudan, T. N. J. I. Edison, D. Chakradhar, N. Karthik, S. Perumal, and Y. R. Lee, *Ceram. Int.*, 2018, **44**, 2869–2883.